

Variable Sampling of the Empirical Mode Decomposition of Two-Dimensional Signals

Anna Linderhed

Image Coding Group, Department of Electrical Engineering, Linköpings Universitet
S-58183 Linköping, SWEDEN

Swedish Defence Research Agency, P.O. Box 1165, SE-581 11 Linköping, Sweden
anna.linderhed@foi.se

Abstract - Previous work on Empirical Mode Decomposition in two dimensions typically generates a residue with many extrema points. In this paper we propose an improved method to decompose an image into a number of Intrinsic Mode Functions and a residue image with a minimum number of extrema points. We further propose a method for the variable sampling of the two-dimensional Empirical Mode Decomposition. Since traditional frequency concept is not applicable in this work we introduce the concept of empiquency, short for Empirical Mode Frequency, to describe the signal oscillations. The very special properties of the Intrinsic Mode Functions are used for variable sampling in order to reduce the number of parameters to represent the image. This is done blockwise using the occurrence of extrema points of the Intrinsic Mode Function to steer the sampling rate of the block. A method of using overlapping 7x7 blocks is introduced to overcome blocking artifacts and to further reduce the number of parameters required to represent the image. The results presented here shows that an image can be successfully decomposed into a number of Intrinsic Mode Functions and a residue image with a minimum number of extrema points. The results also show that subsampling offers a way to keep the total numbers of samples generated by Empirical Mode Decomposition approximately equal to the number of pixels of the original image.

Keywords: Empirical Mode Decomposition, time-frequency analysis, image processing, sampling, sequency, empiquency.

1. Introduction

A relatively new, and promising, technique has been developed to perform general analysis of highly transient time-domain signals, called the Hilbert-Huang Transform (HHT) [1]. It has shown great utility in time-frequency analysis of dispersive, nonlinear, or non-stationary signals and systems. The transform uses the Empirical Mode Decomposition (EMD). The EMD process allows time-frequency analysis of transient signals for which Fourier based methods have been unsuccessful. Whenever we use the Fourier transform to represent frequencies we are limited by the uncertainty principle. For infinite signal length we can get exact information about the frequencies in the signal, but when we restrict ourselves to analyse a signal of finite length there is a bound on the precision of the frequencies that we can detect. Many methods exist to analyse signals in the time- and frequency-domain at the same time, Short-Time Fourier Transform [2], Wigner distribution [2] and Wavelets [3] among others. All these methods are based on the expansion of the signal into a set of basis functions where the basis functions are defined by the method. The concept of the EMD is to expand the signal into a set of functions defined by the signal itself, the Intrinsic Mode Functions (IMF). This is done in such a way that we can use instantaneous frequency for time-frequency analysis. The HHT measures the concept of instantaneous frequency of each of the signal components from the EMD and presents the result as a time-frequency analysis in a Hilbert spectrum plot. No information is lost by the EMD. The signal is decomposed into a redundant set of signals denoted IMF and a residue. Adding all the IMFs together with the residue reconstructs the original signal without information loss or distortion.

HHT, the EMD-based time-frequency analysis, is only one of many applications possible by the use of EMD. In the two-dimensional case, where the adaptive spatial frequency separation presents a challenge, the EMD enables many new approaches for image processing applications.

The EMD is a truly empirical method, not based on the Fourier frequency approach but, as we will see, related to the locations of extrema points and zero-crossings. Based on this we use the concept of *empiquency*, short for empirical mode frequency, instead of a traditional frequency measure to describe the signal oscillations. The measure of empiquency is defined as “One half the reciprocal distance between two consecutive extrema points”.

This paper begins with a review of the EMD applied to time signals as an introduction to the concept. Previous work often mention the lack of a mathematical formalism to describe the EMD, the concept is truly empirical. In this paper we keep the empirical approach as we expand the method to two-dimensional signals, such as images. Some efforts to implement the EMD in two dimensions has been published [5] [6] but the methods typically generates a residue with many extrema points. We will give an example of such an implementation and explain why it does not work. In this paper we also present an improved method that can decompose the image into a number of IMFs and a residue with none, or with only a few extrema points.

The main part of the paper concerns the issue of reducing the number of parameters required to represent the EMD of the image. This is done through variable sampling that takes advantage of the very special properties of the IMFs. These are zero mean and never have more than one extrema point between two neighbouring zero-crossings. This enables us use the empiquency to steer the block based sampling which is the basis for the variable sampling method presented in this paper. Because of the relationship between zero-crossings and extrema points there is also a relation between the empiquency and the concept of *sequency*. Sequency is defined as, “ the average number of zero crossings per second divided by 2” [4]. For a sine or cosine the frequency and the sequency is the same, but the concept of sequency has a meaning for other signals such as Walsh functions or IMFs as well.

2. EMD of time signals

The EMD is a highly adaptive decomposition. It decomposes any complicated signal into so called intrinsic mode functions (IMF). The IMFs lead to a clean representation of the signal by a few well-behaved signal components. Traditional Fourier analysis does not allow a signal's spectrum to change over time. The EMD, however, provides a decomposition method that analyses the signal locally and separates the component holding locally the highest empiquency from the rest into a separate IMF. Within this IMF both high and low empiquencies can coexist at different times. The key word is *locally*.

Time-frequency analysis by means of HHT, or EMD separately, has been done in several areas such as analysis of ocean waves, seismology, and one-dimensional analysis of SAR images[1] [7] [8]. The behaviour of the EMD as a filter bank is highlighted by [9] in the analysis of noise.

An IMF is characterized by some specific properties. One is that the number of zero crossings and the number of extrema points is equal or differs only by one. This way the empiquency of the IMF is defined by the number of extrema points as well as by its zero-crossings. Another property of the IMF is that the envelopes defined by the local maxima and minima, respectively, is locally symmetric around the envelope mean.

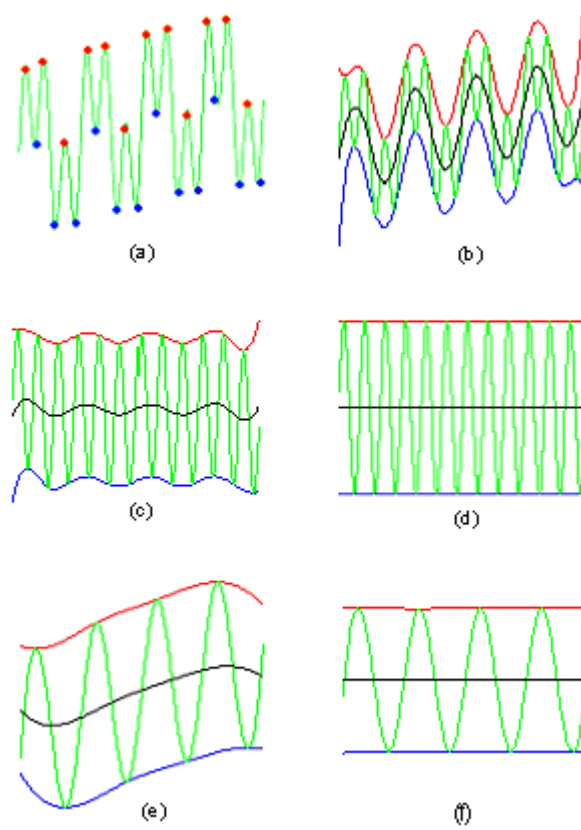


Figure 2.1. a: The test signal with the local maxima marked by red dots and the local minima marked by blue dots, b: the test signal with upper envelope in red, lower envelope in blue and the envelope mean in black. c: the result from one iteration in the IMF sifting process with the upper and lower envelope in red and blue and their mean in black. d: the resulting first IMF with the upper and lower envelope and their mean. e f: Iteration for the second IMF:

The sifting process to find the IMFs is described and visualized by a very simple test signal, the addition of two sine curves and a slowly varying trend, the green curve in Figure 2.1(a) denoted by $x(t)$. The process comprises the following steps:

1. Find all the points of local maxima, and all the points of local minima in the signal. These are marked by red and blue dots respectively in Figure 2.1(a).
2. Create the upper envelope by spline interpolation of the local maxima and the lower envelope by spline interpolation of the local minima of the input signal, shown as the red and blue curves in Figure 2.1(b) denoted $e_{max}(t)$ and $e_{min}(t)$. Cubic spline is used in this example.
3. For each time instant, calculate the mean of the upper envelope and the lower envelope.

$$m(t) = \frac{e_{max}(t) + e_{min}(t)}{2} \tag{1}$$

This signal $m(t)$ is referred to as the envelope mean and is the black line in Figure 2.1(b), 2.1(c), and 2.1(d).

4. Subtract the envelope mean signal from the input signal (black in Figure 2.1(b) from green in Figure 2.1(a)), yielding the results illustrated by green in Figure 2.1(c).

$$h_1(t) = x(t) - m_1(t) \tag{2}$$

This is one iteration of the sifting process. The next step is to check if the signal from step 4 is an IMF or not. In the original work [1] the sifting process stops when the difference between two consecutive siftings is smaller than a selected threshold. In this paper the process stops when the envelope mean signal is close enough to zero.

$$|m(t)| < \varepsilon \quad \forall t \quad (3)$$

The reason for this choice is that forcing the envelope mean to zero will guarantee the symmetry of the envelope and the correct relation between the number of zero crossings and number of extremes that define the IMF.

5. Check if the mean signal is close enough to zero, based upon the stop criterion. If not, repeat the process from step 1 with the resulting signal from step 4 as the input signal a sufficient number of times.

$$h_{11}(t) = h_1(t) - m_{11}(t) \quad (4)$$

$$h_{1k}(t) = h_{1(k-1)}(t) - m_{1k}(t) \quad (5)$$

$$c_1(t) = h_{1k}(t) \quad (6)$$

where the first index is the IMF number and the second index is the iteration number in the sifting process.

After the IMF $c_1(t)$ is found, (here illustrated by the green curve in Figure 2.1(d)), define the residue $r(t)$ as the result from subtracting this IMF from the input signal.

$$r_1(t) = x(t) - c_1(t) \quad (7)$$

The residue is illustrated by the green curve in Figure 2.1(e).

6. The next IMF is found by starting over from step 1, now with the residue as the input signal. The second IMF is illustrated in Figure 2.1(f).

The steps 1 to 6 can be repeated for all the subsequent r_j . The EMD is completed when the residue does not contain any extrema points. This means that it is either a constant or a monotonic function. The conclusion is that the signal $x(t)$ can be expressed as the sum of IMF:s and the last residue

$$x(t) = r_n(t) + \sum_{i=1}^n c_i(t) \quad (8)$$

The first IMF captures the highest empiquency in the signal as a function of time. The range of empiquencies contained in all the IMFs varies over time but the first IMF always contains the locally highest one in the signal.

3. EMD of two-dimensional signals

The results and ideas in time domain applications using the EMD technique apply to two-dimensional signals, such as images, as well. In a similar way as with the one-dimensional EMD, the first IMF extracts the locally highest spatial empiquencies in the image while the second IMF holds the locally next highest spatial empiquencies, etc. The use of the Hilbert transform for the creation of analytic signals in two dimensions is made possible by the introduction of a direction of reference in the Fourier domain [10]. In the two-dimensional EMD, the symmetry criterion on the IMF envelopes is relaxed. The stop criterion is based on the condition that the IMF envelope mean must be close enough to zero. This guaranties that we will find the IMF without actually checking for symmetric envelopes.

3.1 Interpolation for EMD

The EMD in two dimensions relies on proper spline interpolation in two dimensions. Some efforts to implement the EMD in two dimensions have been published [5] [6] but the methods have not proven to be able to fully decompose the two-dimensional signal down to a residue with a low number of extrema points. We will give an example of such an implementation and explain why it does not work. The residue signal should have only a few extrema points, [1] states that there should be no extrema points in the one-dimensional case and ideally we would like to have a similar criterion in the two dimensions. A tutorial on the subject of EMD in both one and two dimensions can be found in [11].

The problem is to fit a surface to the two-dimensional scattered data points representing the extrema points. The interpolated surface must go through each data point. Overshoot shall be avoided and the second derivative must be continuous everywhere for the signal to be smooth enough for two-dimensional EMD. The interpolation methods considered here are triangle-based cubic spline interpolation and thin-plate smoothing spline interpolation. The first is an example of an interpolation method using a piecewise approach to interpolate the surface. It produces piecewise smooth surfaces and is based on Delaunay triangulation [12] of the data. The piecewise approach causes more problems in the two-dimensional case than with one-dimensional signals. Even though the interpolator have continuous second derivatives, such as the cubic spline in [5] or the radial basis functions used in [6], along the borders of the neighbouring pieces the second derivative is not continuous in all directions.

A suggestion for two-dimensional EMD analysis that gives a surface with continuous second derivative everywhere, is to use thin-plate smoothing spline interpolation. The thin-plate smoothing spline algorithm [13] calculates the function f that minimizes the integral bending norm I_f , in equation (9), for given scattered data in the plane. The integral is taken over the entire image, and involves the second derivatives of f .

$$I_f = \iint_{R^2} \left(\left(\frac{\partial^2 f}{\partial x^2} \right)^2 + 2 \left(\frac{\partial^2 f}{\partial x \partial y} \right)^2 + \left(\frac{\partial^2 f}{\partial y^2} \right)^2 \right) \partial x \partial y \quad (9)$$

This means that the determination of the smoothing spline involves the solution of a linear system with as many unknowns as there are data points. This method turns out to successfully decompose an image into its IMFs and a smooth residue with none or only a few extrema points.

The scattered extrema points from the third IMF in Figure 3.3 is shown in Figure 3.1a. Local maxima are plotted as light pixels and local minima are plotted as dark pixels. The different surfaces achieved when interpolating the same scattered data points using thin-plate interpolation and triangle-based cubic interpolation are shown in Figure 3.1b and 3.1c. The effects of using a piecewise approach on very sparse data is obvious from the example.

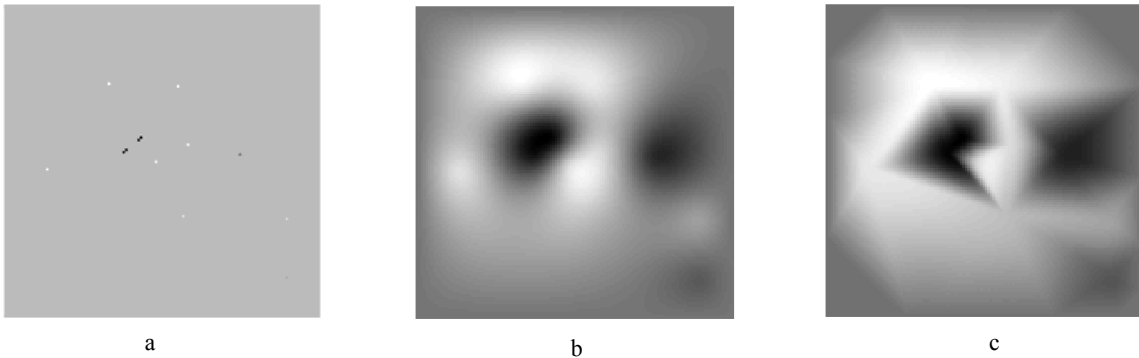


Figure 3.1. The different resulting surfaces when interpolating the scattered data points (a), using thin plate interpolation (b), and triangle-based cubic interpolation (c).

3.2 Finding extrema points and edge constraints

Since we are only concerned with discrete two-dimensional signals the extrema points are simply extracted by comparing the candidate data point with its nearest 8-connected neighbors.

The border constraints are even more important in two dimensions than they are in the one-dimensional EMD case. One of the main objections for using spline interpolation in the EMD for two-dimensional signals such as images is that the borders cause too much problems. The set of extrema points are very sparse and since the interpolation methods only interpolate between points, the borders need special care. The trick is to add extra data points at the borders to the set of extrema points. The extra points are placed at the corners of the image and some additional points at the border equally spaced between the corners. Without these extra points, the areas not covered by the interpolation traverses into the image in the sifting process.

3.3 Example Image EMD

As an example of an image EMD we look at the well-known Lenna image, shown in Figure 3.2. The image's four IMFs and their corresponding residues are shown in Figure 3.3.



Figure 3.2. lenna128.

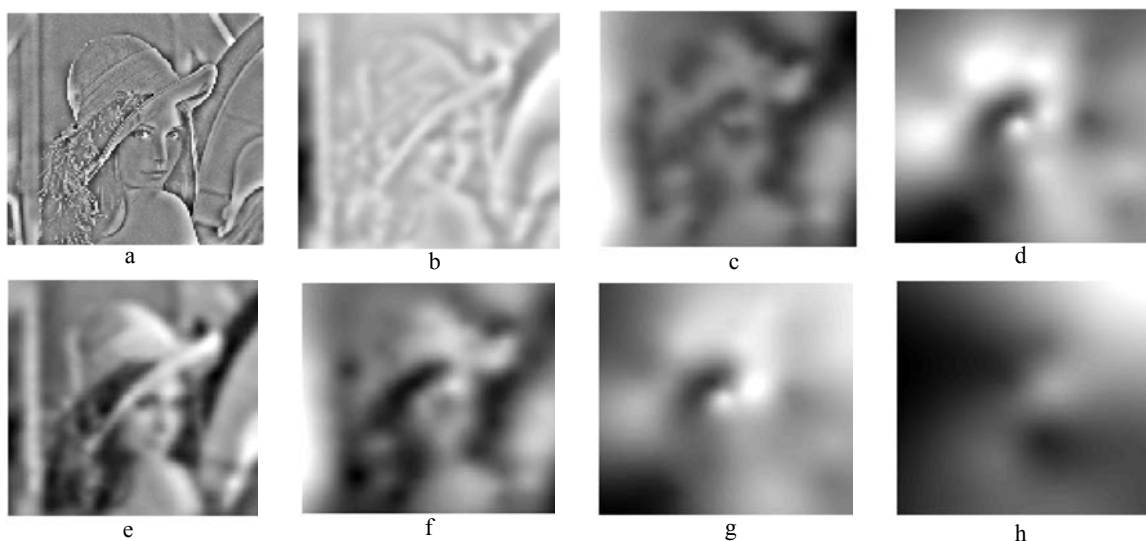


Figure 3.3. a) first IMF, b) second IMF, c) third IMF, d) fourth IMF, e) first residue, f) second residue, g) third residue, h) fourth residue.

It should be noted that all the IMFs are zero mean while the DC level of the signal is contained in the residue. All the IMFs have the very special property of having only one extrema between two zero-crossings in any direction. This will be used in the next section to get a more efficient representation.

4. Sampling of the IMF

The IMFs are smoother than the image itself, only the first IMF holds the nonsmooth parts of the image. This means that it should be possible to subsample the IMFs. Due to the different empiquencies in the different parts of the IMF, the subsampling can be different in different parts of the IMF.

The zero crossings of the IMF define the dominating empiquency. This means that between two consecutive zero crossings there exists only one half period of a possibly periodic function. The shape of the curve of the IMF signal between these two zero crossings is not necessarily a pure sine but can have various shapes.

4.1 Noise reduction

It is sometimes assumed that the first IMF contains all the noise in the signal and that the noise can be removed by just skipping the first IMF. This is not true. Noise usually contains all empiquencies, both higher and lower than the maximum spatial empiquency of the signal. For signals with moderate signal-to-noise ratio, we can assume that the noise is of lower amplitude than the extrema points. Then we can reduce the noise by setting the extrema points with low amplitude to zero. Figure 4.1 shows the extrema points of the first IMF and the histogram of the same. As can be seen, most of the pixels are already zero because they are not extrema points.

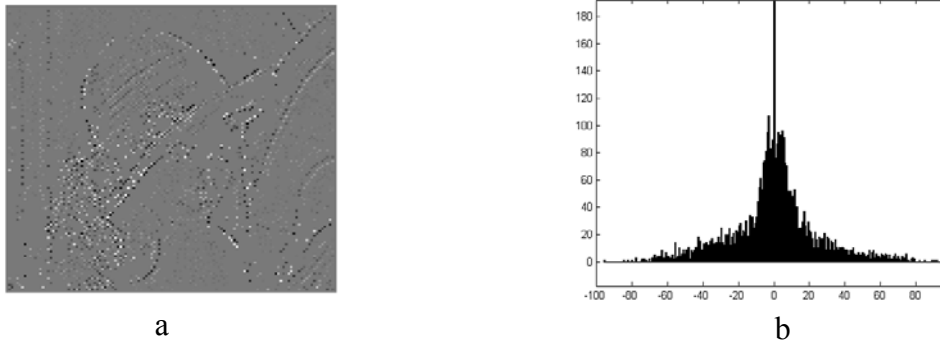


Figure 4.1. a) The extrema points of the first IMF, b) zoomed histogram of the extrema points of the first IMF.

If we let the coefficients with absolute amplitude lower than a suitable threshold, in this case 10, be set to zero we get the result shown in Figure 4.2 .

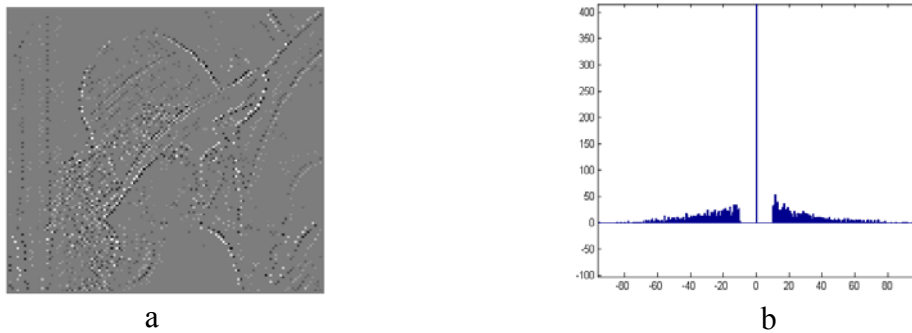


Figure 4.2. a) The extrema points with the smallest coefficients set to zero, b) histogram of the extrema points with the smallest coefficients set to zero.

This noise reduction introduces errors into the original signal. The reconstructed image will be distorted, which will show up in the SNR measure.

4.2 Variable sampling

The special properties of the IMF that the empquency varies can be used for variable sampling. Areas with many extrema points have high empquency while areas with a few or no extrema points have low empquency. Maximum empquency is found by examining the space between the extrema points. Figures 4.3 and 4.4 shows two discrete time signals, both with the properties of an IMF but with different maximum empquency, (0.5, in a normalized scale, for the signal in Figure 4.3 and 0.167 for the signal in Figure 4.4). We expect that the signal example in Figure 4.4 can be

reconstructed with low distortion from a subsampled version, while the signal example in Figure 4.3 needs every sample to be represented without distortion due to its high maximum empiquency.

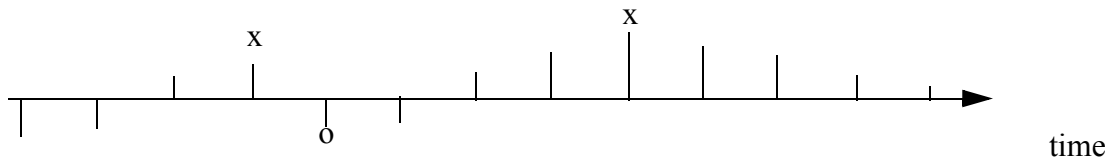


Figure 4.3. A discrete time signal with its three extrema points marked with “x” for local maxima and “o” for local minima. Maximum empiquency 0.5..

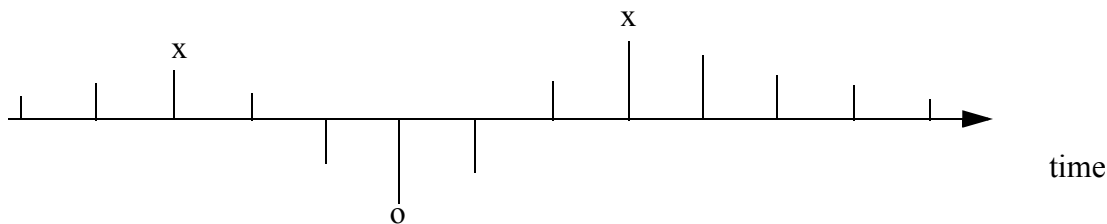


Figure 4.4. A discrete time signal with its three extrema points marked with “x” for local maxima and “o” for local minima. Maximum empiquency 0.125.

It is known [14] that a band-limited signal can be uniquely determined from its non-uniform samples, provided that the average sampling rate exceeds the Nyquist rate. For an image containing spatial frequencies up to half this value the image cannot be reconstructed without distortion if it is subsampled. We let the extrema points define the maximum empiquency in the IMF. In the first IMF there are areas where every pixel is an extrema point, thus the maximum empiquency is 0.5. Letting this define our Nyquist bandwidth, we expect that it is not possible to subsample this IMF without distortion.

Our suggestion is to treat the IMF blockwise. The sampling rate is defined by the maximum empiquency in the block. Again we expect all lower empiquencies to be represented without distortion. This way the sampling rate for each block can be defined according to its empiquency content. The high empiquency blocks which cannot be subsampled according to Nyquist are not modified. The remaining ones are subsampled.

4.3 Reconstruction

For a signal $f(t)$ that is band limited to $\left[-\frac{1}{2T}, \frac{1}{2T}\right]$ and sampled according to the sampling theorem, the signal can be reconstructed without distortion from its sampled version $f(nT)$ through the reconstruction formula

$$f(t) = \sum_{n=-\infty}^{\infty} f(nT)h_T(t-nT) \quad (10)$$

A sampling function $h_T(t)$ used for reconstruction satisfies

$$h_T(t) = \begin{cases} 1 & \text{if } t = 0 \\ 0 & \text{if } t = nT \end{cases} \quad (11)$$

The sampling function that should be used according to the sampling theorem is the cardinal basis function $sinc(t)$.

$$h_T(t) = \frac{\sin(\pi t/T)}{(\pi t/T)} \quad (12)$$

This theory relies on the use of ideal filters. The use of finite signals is however in contradiction to the band limitation approach. An alternative approach is to use splines. These are piecewise polynomials where the pieces are smoothly connected together at the sample points.

The cubic spline interpolator is given by

$$b^{(3)} = \begin{cases} \frac{2}{3} - \left|\frac{t}{T}\right|^2 + \frac{\left|\frac{t}{T}\right|^3}{2} & 0 \leq \left|\frac{t}{T}\right| < 1 \\ \left(2 - \left|\frac{t}{T}\right|\right)^3 & 1 \leq \left|\frac{t}{T}\right| < 2 \\ 0 & 2 \leq \left|\frac{t}{T}\right| \end{cases} \quad (13)$$

The cardinal cubic spline function, shown in Figure 4.5, represents the impulse response of the corresponding spline interpolator [15]. This function vanishes at all integer positions except at the origin and thus has the same interpolation properties as the sinc function.

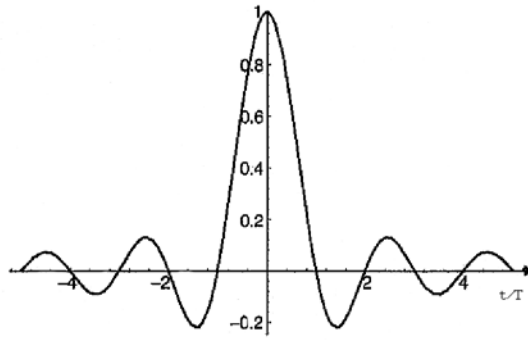


Figure 4.5. Cubic spline sampling function.

Considering the fact that we are treating finite signals, the use of the spline interpolator to reconstruct the image from its samples is superior to using a windowed sinc function as interpolator. The uniformly sampled points of the block are thus connected by a surface created by the use of an interpolating cubic spline extended to two dimensions.

4.4 Overlapping blocks

In the implementation of the block reconstruction we choose to use overlapping blocks of size 7x7 pixels. This is to minimize the artifacts from the blocking and to further reduce the samples used to represent the IMF. The overlapping pixels in the two blocks will be the same, but used twice, this will ensure that the concatenated blocks have the same values at the edge pixels. The overlapping pixels will only belong to one of the blocks when patching and counting the total number of samples.

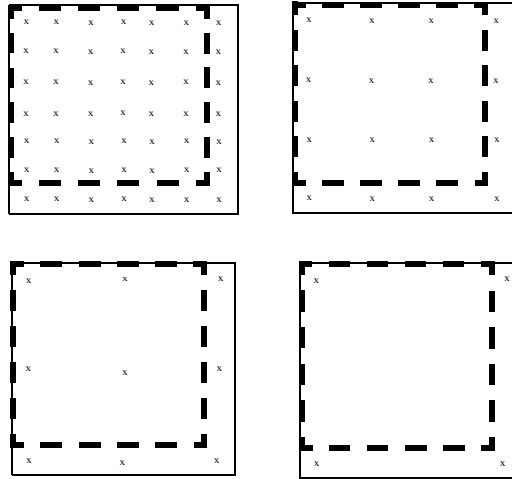


Figure 4.6. Variable sampling with overlapping 7x7 blocks.

We further assume that the maximum empiquency is the same horisontally and vertically within the block. Sampling rates are 1, 2, 3 and 6 to represent every pixel, 1/4, 1/9, 1/36 of the samples respectively.

Reconstruction of the image uses the 7x7 block for block reconstruction with interpolation. The nonoverlapping 6x6 part of the reconstructed block is used for patching the blocks together to the image.

5. Result

Reconstructing the subsampled blocks is done with cubic interpolation over a regular set of samples. The SNR measure is computed from the original and the reconstructed image. The average sampling rate measure is a count of the number of samples used in relation to the total number of pixels in the image. The sum of samples to represent all of the IMFs and the residue is 14023 corresponding to a sampling rate of 0.86. The image is reconstructed by the sum of IMFs and residue with the distortion of 31.8 dB. The result of the variable subsampling of the example in terms of samplingrate and distortion is presented in the tabel in Figure 5.1.

	Sampling rate	Distortion
Image	0.86	31.80 dB
IMF1	0.64	33.04 dB
IMF2	0.123	42.31 dB
IMF3	0.035	40.83 dB
IMF4	0.029	50.20 dB
residue 4	0.028	61.63 dB

Figure 5.1. The result of the variable subsampling of the example in terms of sampling rate and distortion.



Figure 5.2. Reconstructed image by the sum of IMFs and residue, 31.8 dB using an average sampling rate of 0.86.



Figure 5.3. IMF1 33.0414dB using 10500 coefficients corresponding to an average sampling rate of 0.64.

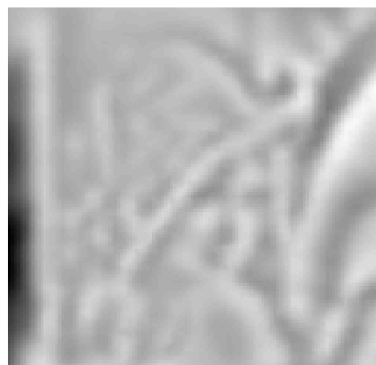


Figure 5.4. IMF2 42.3124dB using 2020 coefficients corresponding to an average sampling rate of 0.123.



Figure 5.5. IMF3 40.8331 dB, 576 coefficients corresponding to an average sampling rate of 0.0352.

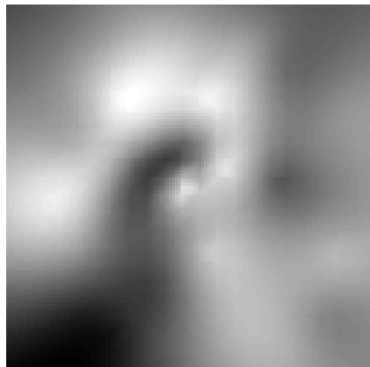


Figure 5.6. IMF4 50.2062 dB, 474 coefficients corresponding to an average sampling rate of 0.029.

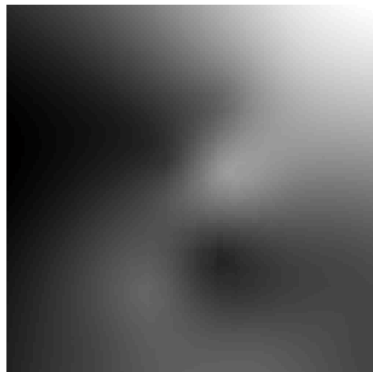


Figure 5.7. residue4 61.6378 dB, 453 coefficients corresponding to an average sampling rate of 0.028.

6. Conclusion

In summary the EMD is an interesting approach to decompose signals into locally periodic components, the intrinsic modes. We have shown how to decompose a full image EMD into a number of IMFs and a residue image with no, or a minimum number of, extrema points. We have proposed a method for variable sampling of the two-dimensional EMD. We introduce the concept of

empiricity, short for empirical mode frequency, to describe the signal oscillations, since traditional frequency concept is not applicable in this work. The very special properties of the IMF is used for variable sampling of the IMFs and the residue in order to reduce the number of parameters to represent the image. This is done blockwise using the non-uniformly located extrema points of the IMF to steer the uniform sampling rate of the block. Possible improvements to the scheme would be to determine the sampling rate for each block by a rate-distortion approach, comparing the result from using all the sampling rates on each block. Also, different rates horizontally and vertically can be introduced. A method of using overlapping 7x7 blocks is introduced to overcome blocking artifacts and to further reduce the number of parameters to represent the image. The results presented here shows that subsampling offers a way to keep the total numbers of samples generated by EMD approximately equal to the number of pixels of the original image.

7. References

- [1] N. E. Huang et al. "The empirical mode decomposition and the Hilbert spectrum for nonlinear and non-stationary time series analysis". Proc. R. Soc. Lond. A (1998) 454, 903-995.
- [2] Leon Cohen, Time -Frequency Analysis, Prentice Hall, ISBN 0-13-594532-1.
- [3] Stéphane Mallat. A wavelet tour of signal processing, second edition. Academic Press. 1999. ISBN 0-12-466606-X.
- [4] Henning F. Harmuth, Transmission of Information by Orthogonal Functions, Springer-Verlag Berlin/Heidelberg 1969.
- [5] Anna Linderhed, "2D empirical mode decompositions in the spirit of image compression", Wavelet and Independent Component Analysis Applications IX , SPIE Proceedings Vol. 4738, pp.1-8, April 2002, ISBN: 0-8194-4488-X.
- [6] J. C. Nunes, , Y. Bouaoune, E. Delechelle, O. Niang and Ph. Bunel, Image analysis by bidimensional empirical mode decomposition, Image and Vision Computing, Volume 21, Issue 12 , November 2003, Pages 1019-1026.
- [7] Kris Vasudevan, Frederick A. Cook, "Empirical mode skeletonization of deep crustal data: Theory and applications", Journal of Geophysical research, vol 105, no B4, april 2000.
- [8] Yue Huanyin et.al, "A SAR Interferogram Filter Based on the Empirical Mode Decomposition Method", IGARSS 2001. Scanning the Present and Resolving the Future. Proceedings. IEEE 2001 International Geoscience and Remote Sensing Symposium , 9-13 July 2001 , Sydney, NSW, Australia.
- [9] Patrick Flandrin, Gabriel Rilling, Paulo Goncalves, "Empirical Mode Decomposition as a Filter Bank", Preprint IEEE Signal Processing Letters, 2003.
- [10] Gösta H. Granlund, "Signal Processing for Computer Vision", Kluwer Academic Press 1995, ISBN 0-7923-9530-1.
- [11] Anna Linderhed, "Empirical Mode Decomposition (EMD) in One and Two Dimensions", Submitted to IEEE Signal Processing Magazine.

- [12] Franco P. Preparata , Michael I. Shamos, Computational geometry: an introduction, Springer-Verlag New York, Inc., New York, NY, 1985.
- [13] Fred L. Booksstein, “Principal warps: Thin-plate splines and the Decomposition of deformations”, IEEE Trans. on Pattern analysis and machine intelligence, vol 11, no 6 june 1989.
- [14] Marvasti, F. Nonuniform sampling theorems for bandpass signals at or below the Nyquist density, IEEE Transactions on Signal Processing, Volume: 44 Issue: 3 , March 1996 Page(s): 572 -576.
- [15] M. Unser. Spline, A Perfect Fit for Signal and Image Processing. IEEE Signal Processing Magazine, Nov 1999.